



Inchworm stepping of Myc-Max heterodimer protein diffusion along DNA

Liqiang Dai ^a, Jin Yu ^{b,*}

^a Beijing Computational Science Research Center, Beijing, 100193, China

^b Department of Physics and Astronomy, Department of Chemistry, NSF-Simons Center for Multiscale Cell Fate Research, University of California, Irvine, CA, 92697, USA



ARTICLE INFO

Article history:

Received 25 July 2020

Accepted 2 August 2020

Available online 12 September 2020

Keywords:

Transcription factor

Facilitated diffusion

Coarse-grained simulation

Molecular dynamics

Myc-Max heterodimer

ABSTRACT

Oncogenic protein Myc serves as a transcription factor to control cell metabolisms. Myc dimerizes via leucine zipper with its associated partner protein Max to form a heterodimer structure, which then binds target DNA sequences to regulate gene transcription. The regulation depends on Myc-Max binding to DNA and searching for target sequences via diffusional motions along DNA. Here, we conduct structure-based molecular dynamics (MD) simulations to investigate the diffusion dynamics of the Myc-Max heterodimer along DNA. We found that the heterodimer protein slides on the DNA in a rotation-uncoupled manner in coarse-grained simulations, as its two helical DNA binding basic regions (BRs) alternate between open and closed conformations via inchworm stepping motions. In such motions, the two BRs of the heterodimer step across the DNA strand one by one, with step sizes reaching about half of a DNA helical pitch length. Atomic MD simulations of the Myc-Max heterodimer in complex with DNA have also been conducted. Hydrogen bond interactions are revealed between the two BRs and two complementary DNA strands, respectively. In the non-specific DNA binding, the BR from Myc shows an onset of stepping on one association DNA strand and starts detaching from the other strand. Overall, our simulation studies suggest that the inchworm stepping motions of the Myc-Max heterodimer can be achieved during the protein diffusion along DNA.

© 2020 The Authors. Published by Elsevier Inc. This is an open access article under the CC BY-NC-ND license (<http://creativecommons.org/licenses/by-nc-nd/4.0/>).

1. Introduction

Gene expression relies essentially on transcription factors (TFs) search on DNA to locate sequence motifs for subsequent regulation protein association and assembly. During the search process, the TF protein often binds to non-specific DNA and then approaches to a specific DNA binding site via diffusion on the DNA [1,2]. A facilitated diffusion model had been suggested in which TFs alternate between 3-D cellular space diffusion and 1-D diffusion along DNA in order to achieve efficient target search and binding [1,3–7]. In 1-D diffusion, TF can track, slide, and hop along DNA. It can also jump for intersegmental DNA transfer.

Although phenomenological models of the facilitated diffusion have been established [1,3–7], molecular details of the TF diffusion remain largely unknown. Single molecule experiments could detect TF diffusional motions on the DNA [8–10], yet it is highly

challenging to capture the movements at base-pair (bp) spatial resolution or sub-millisecond time resolution. In comparison, motor proteins can be slowed down in a controllable manner (e.g. by reducing ATP concentration) to allow high-resolution detection. For example, real-time single-molecule measurements demonstrated hand-over-hand stepping motions of kinesin or myosin motors along microtubules or actin filaments [11–14]. Single bp movements of nucleic acid motors such as RNAP polymerase [15] or DNA helicase along DNA track have also been identified [16,17].

On the other hand, structure-based simulations allow for molecular dynamics (MD) characterization of key structure components of the systems. Atomic MD simulations contain finest structural dynamics details but are often limited by the simulation time scale, which can hardly surpass several microseconds for a TF protein-DNA system of a regular size [18–20]. Coarse-graining (CG) techniques, however, provide ways to extend the simulation time scale via maintaining essential protein-DNA electrostatic interactions to support the TF diffusion [21–24]. In current studies implementing the CG simulations using CafeMol [25], each protein amino acid is represented by one bead, and each DNA nucleotide is

* Corresponding author.

E-mail address: jin.yu@uci.edu (J. Yu).

modeled by three beads [26]. Similar simulation studies have demonstrated rotation-coupled or uncoupled sliding motions of TFs along DNA [22,27,28].

Here, we employed mainly the protein-DNA structure-based CG simulations to investigate diffusional motions of a heterodimer TF Myc-Max on the DNA. Myc plays an important role in cell proliferation, differentiation, and apoptosis. Deregulated level of Myc leads to abnormal cell growth or cancer [29–31]. Myc cannot form a homodimer under physiological condition, instead, it forms a heterodimer with the Myc-associated-factor X (Max) for most of its known functions [32–34]. The Myc-Max heterodimers can specifically bind to cognate DNA sequences (e.g. 5'-CACGTG-3') termed the enhancer box or E-box [32]. In regular conditions, Myc-Max binds mostly to the E-box and consensus sequences populated in active promoter regions [35].

The Myc family members contain a N-terminal transactivation domain, a middle segment rich in proline, glutamic acid, serine, and threonine residues (PEST), and a C-terminus basic region/helix-loop-helix/leucine zipper (bHLHLZ) domain [36,37]. The N-term and PEST domain of Myc are largely disordered. The well-folded molecular structure of the bHLHLZ domain is presented in Fig. 1A [38]. The Myc/Max monomer structure thus contains the DNA-bounded basic region (BR), the helix-loop-helix (HLH) motif, and the leucine zipper (LZ) domain that serves as an anchor to stabilize the dimer structure [38,39]. The presented structure appears to be in a closed state. An open conformation of homodimer Max-Max has also been suggested [40].

Computational studies have been conducted mostly toward Myc-Max inhibition for drug discovery approaches [41–43]. The dimerization specificity of c-Myc had been modeled [44]. Modeling also shows different promoter binding affinities accounting for Myc gene regulation specificity [45]. In this work, we focus on characterizing diffusional motions of the Myc-Max heterodimer along nonspecific DNA. To do that, we conducted the structure-based CG simulations, in which the protein-DNA electrostatic interactions are largely maintained. We found that Myc-Max diffuses on the DNA via 1-D sliding motions. The heterodimer transits between two dominant conformations (closed and open), and two DNA binding BRs alternately step across the DNA strand in rotation-uncoupled and inchworm motions [46,47]. Additional atomistic MD simulations up to 1 μ s each have also been conducted for Myc-Max in complex with specific and non-specific DNA. Initial stepping and DNA strand detachment of Myc show in the non-specific DNA binding.

2. Results

2.1. The rotation uncoupled sliding of the Myc-Max heterodimer along DNA

We conducted CG simulations to investigate the Myc-Max diffusion along DNA. The CG protein was built by using the G^0 model [48], with each amino acid represented by one bead. The CG DNA is built by 3SPN2C model [26], with each nucleotide represented by 3 beads, corresponding to sugar, base and phosphate, respectively (Fig. 1A bottom). The simulation was conducted for 5×10^8 time steps ($\sim 10 \mu\text{s}$ [25] as a lower bound estimation) under a physiological ionic strength (150 mM). The center of mass (COM) of two BRs of protein is initially placed 25 \AA above DNA, then the protein quickly binds to the DNA and starts diffusing along the DNA in the simulation (see Supplementary Information or SI Fig. S1). The positioning of the COM of the protein BRs is measured (Fig. 1B left). The protein moves and rotates occasionally around the DNA during sliding in both directions (i.e., +Y toward right and -Y left). Although the Myc-Max heterodimer could rotate around the DNA from time

to time, the correlation between the protein longitudinal diffusing/sliding on the DNA (ΔY) and the rotational ($\Delta\theta$) per 1000 timesteps appears low (correlation coefficient = 0.16; Fig. 1B right). Hence, the sliding of Myc-Max is rotationally uncoupled. To further determine the diffusion rate of the protein along DNA, two additional CG simulations were conducted (Fig. 1C left). The mean square displacements (MSDs) of the COM of protein BRs along DNA are shown (Fig. 1C right), with a diffusion coefficient fitted to $\sim 23 \text{ nm}^2/\mu\text{s}$. Note that the diffusion coefficient can be overestimated due to lack of detailed interactions between protein and DNA in the CG simulations.

Besides, how fast Myc-Max diffuses along DNA also depends on the ionic condition. Under a low ionic strength, due to weak charge screening, the protein is bound tightly to the DNA. Interestingly, we notice that the dimer may dissociate into two monomers, which slide independently along DNA in the CG simulations (see SI Fig. S2A). Previous studies did show for kinetic preference that Myc and Max monomers can bind DNA first and then dimerize [49]. Under a high ionic strength, with comparatively strong charge screening from the solution (implicitly modeled; see SI Methods) on the protein-DNA association, the protein may occasionally dissociate from DNA (SI Fig. S2B).

2.2. Dominant conformational changes of Myc-Max during diffusion along DNA

The sliding of the Myc-Max heterodimer is however coupled closely to significant conformational changes between the two BRs. We measured the distance between the two BR COMs of Myc and Max along DNA as dY (see Fig. 2A left). Within a long period of time, a certain 'left-right' positioning of the Myc-Max BRs is maintained (e.g. $dY > 0$ for Myc/Max keeping right/left lasts for 7.5×10^5 timesteps).

For a complete CG simulation 1, we found that $dY(t)$ is not simply a two-state time series, but is composed of mainly six states (Fig. 2A right; with labels 1-2-3 for $dY > 0$ and 1'-2'-3' for $dY < 0$). The histogram of dY from the full simulation is shown (Fig. 2B). There are four significant peaks and two insignificant but visible ones in the histogram, referring to three inter-BR conformations (closed for 1 and 1', open for 2 and 2', and tightly closed for 3 and 3'): (1) The closed state ($|dY| \sim 20 \pm 3.5 \text{ \AA}$) resembles the crystal structure [38], with the two BRs bound on the two sides of a same DNA groove; (2) the open state ($|dY| \sim 33 \pm 4.2 \text{ \AA}$) is reached as the leading BR moves across the DNA strand and binds to the next DNA groove, by starting from the closed state; (3) the tightly closed state ($|dY| \sim 6.5 \pm 4.4 \text{ \AA}$) is obtained as the lagging BR moves further close to the leading BR, also starting from the closed state. The closed state accounts dominantly for $\sim 63\%$ of the overall population, with an average duration time $\sim 4.1 \times 10^5$ steps (see Fig. 2C); the open state accounts $\sim 28\%$, with a duration time $\sim 2.5 \times 10^5$ steps; and the tightly closed state accounts $< 10\%$, with a duration time $\sim 0.9 \times 10^5$ steps.

2.3. An inchworm stepping model of the Myc-Max heterodimer diffusion along DNA with stochastic left-right reversal

Correspondingly, we suggest that the Myc-Max heterodimer diffusion along DNA follows an inchworm model (see Fig. 3A), moving either forward or backward (see Supplementary Movie S1/S2). Starting from the highly populated closed conformation (state 1), the leading BR moves forward first across the DNA strand to the next DNA groove, at a step size of $\sim 13 \text{ \AA}$, so that Myc-Max transits to the open conformation (state 2); then the lagging BR follows to recover the protein back to the closed state. Such BR stepping motions represent typically the inchworm type of domain/

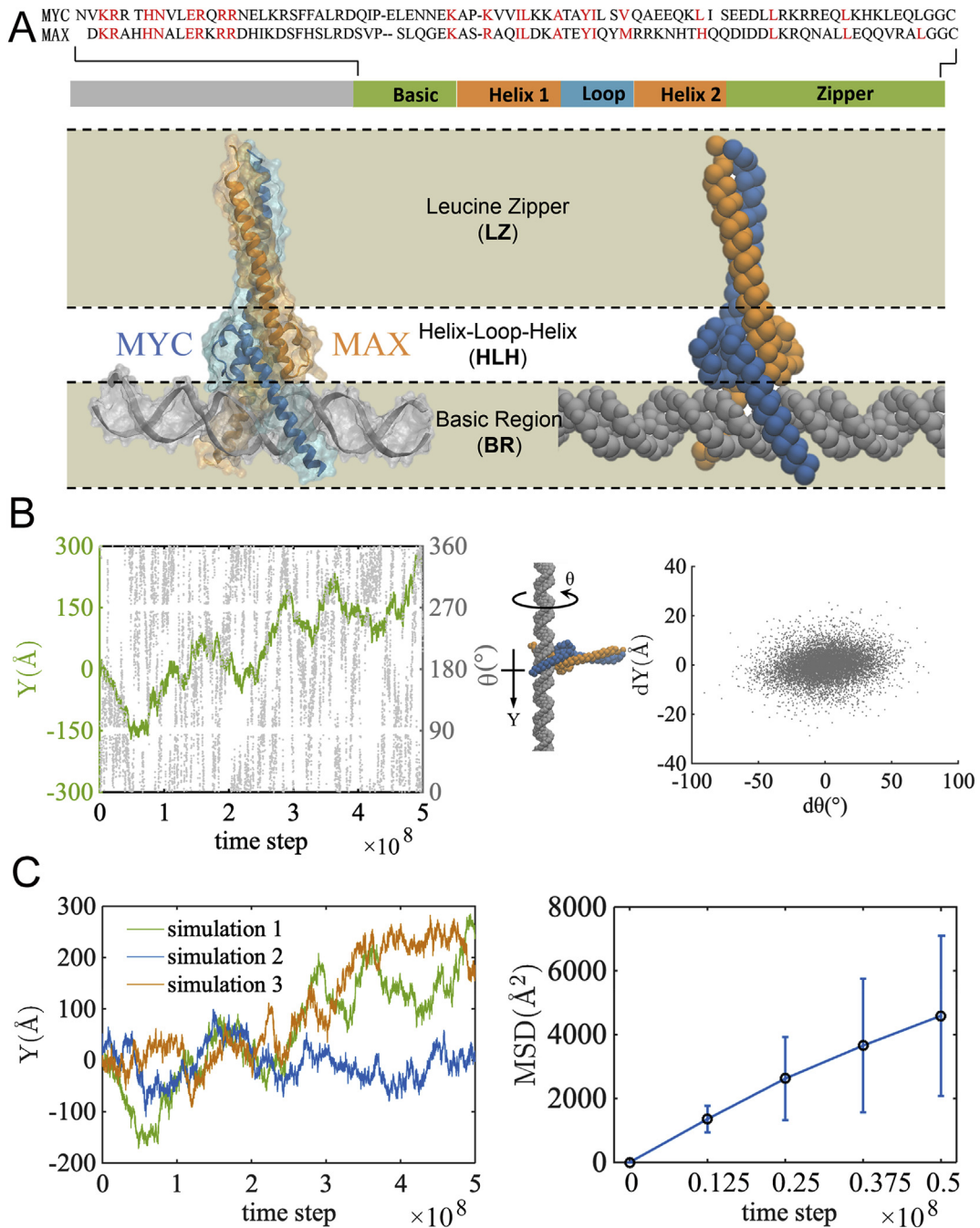


Fig. 1. Coarse-grained (CG) simulations of the Myc-Max heterodimer diffusing along DNA. (A) The Myc and Max protein sequence alignment is shown and the conserved residues are highlighted in red (top). The molecular view of the heterodimer in complex with DNA (pdb: 1NKP) [38] is shown (bottom left), with Myc, Max, and DNA colored in blue, orange, and gray, respectively. The CG structure of the complex is also shown (bottom right). (B) The center of mass (COM) positioning of Myc-Max BRs mapped on the DNA. The DNA long axis is aligned to the Y-axis. The position of the protein along the DNA is shown by green line, and the protein rotational degree around the DNA is shown in gray dots (left). For every 1000 timesteps, 2D mapping of the longitudinal distance ΔY and the rotational degree $\Delta\theta$ is shown (right). (C) The diffusion of the protein along DNA. The COM of the BRs along the DNA for three independent runs are shown (left). The mean square displacements (MSDs) of the protein COM vs the time is also presented for the simulations (right). (For interpretation of the references to color in this figure legend, the reader is referred to the Web version of this article).

subdomain motions [46,47]. Besides, it seems that the protein BR movements along DNA are also correlated well with fluctuations of DNA, as the BR detaches from the DNA for the movements (see SI Figs. S3A and B). Meanwhile, no correlation has been found between the local bending of the DNA and the binding of protein (see SI Fig. S3C).

Occasionally, starting from the closed state, the lagging BR can also move forward first. In such a case, the heterodimer transits to

the tightly closed state (state 3), which is of low population and shortly lived. Rather than transiting back to the stabilized closed state, the tightly closed state allows the BR 'swapping' so that the left-right positioning between the two BRs exchanges or reverses. Such BR swapping events (e.g. 134 caught in the 5×10^8 simulation timesteps; see Supplementary Movie S3) stochastically intervene the regular inchworm sliding. Followed by the BR swapping, the other closed state (1') with an opposite left-right positioning is

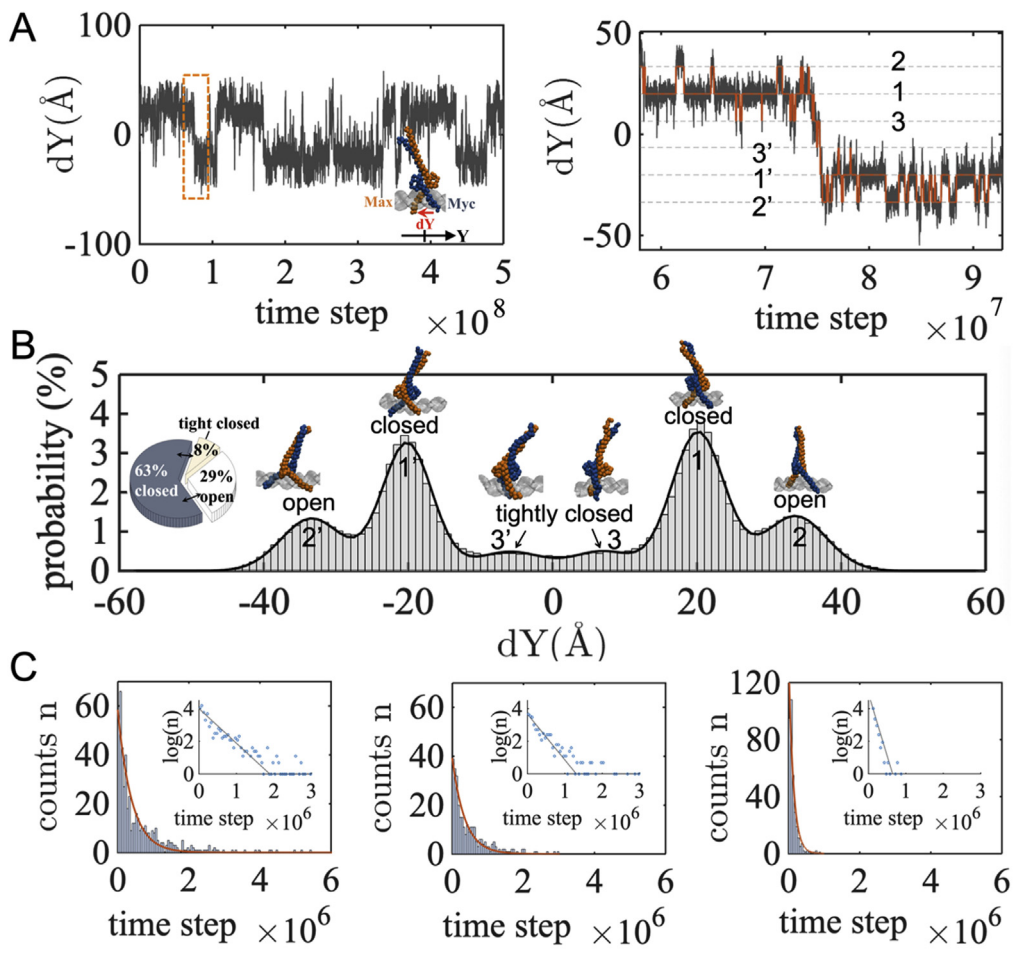


Fig. 2. Various inter-BR conformations of Myc-Max during diffusion along DNA. (A) The distance vector dY between the COMs of the two BR domains of Myc and Max chain is mapped along the DNA during the CG simulation 1 (left). The zoom-in view of the trajectory within an orange rectangle is shown (right). Six states are labeled, three for $dY > 0$ (1, 2, and 3) and three for $dY < 0$ (1', 2', and 3'). (B) The histogram of the distance vector dY between the Myc and the Max BRs is shown, with a representative conformation for each peak illustrated. (C) The survival conformational counts over time steps for the open, closed, and tightly closed states measured from the simulation 1, the average survival or duration time for each conformation is obtained. To compare the survival conformation accounts with an exponential decay function of the time in a Poisson process, the log of the counts vs. time is shown in the inset, with the line a linear fit as an approximation. (For interpretation of the references to color in this figure legend, the reader is referred to the Web version of this article).

reached, via protein self-rotation and two intermediate states (I and II, see Fig. 3B bottom). To check whether the swapping is conformationally reasonable at atomic resolution, we also converted the key CG conformations (from Fig. 3B) to the all-atom representation (structures available upon request). The atomic structures were then morphed via geometrical interpolations and energy minimizations into one trajectory (shown via *Supplementary Movie S4*).

Supplementary video related to this article can be found at <https://doi.org/10.1016/j.bbrc.2020.08.004>

Furthermore, it is noted that overall the probabilities for Myc and Max becoming a leading chain in the diffusion keep the same (see SI Fig. S4). It is equally likely for Myc-Max to move forward and backward, and it is also equivalent to place Myc and Max left or right in the heterodimer on the double-stranded (ds)DNA without structure or sequence bias.

2.4. Binding and onset of diffusion of Myc-Max on DNA in atomistic MD simulations

Although the CG simulations capture essential protein-DNA

electrostatic interactions, the hydrogen bond (HB) interactions formed at the protein-DNA interface are missing. To include those detailed interactions and probe protein-DNA association dynamics, we conducted respective 1- μ s atomistic MD simulations for Myc-Max binding onto specific (E-box) and nonspecific (poly-AT) DNA sequences. Myc-Max shows larger fluctuations on the poly-AT DNA than on the E-box (see SI Fig. S5).

In the atomistic simulations, the Myc and Max BRs are able to form similar amounts of HBs with two complementary DNA strands, respectively (see SI Part 2 and Figs. S6 and S7). Notably, in the non-specific DNA binding, stepping of Myc on an associated polyAT strand is initiated (toward 5' direction). Meanwhile, detachment of the Myc BR from the less associated DNA strand has been found. Both the initial stepping and the strand dissociation of Myc are expected to facilitate further protein diffusion.

3. Discussion

By conducting protein structure-based simulations, we show that diffusion of the Myc-Max heterodimer along DNA can be achieved via inchworm stepping. The two BRs of Myc-Max

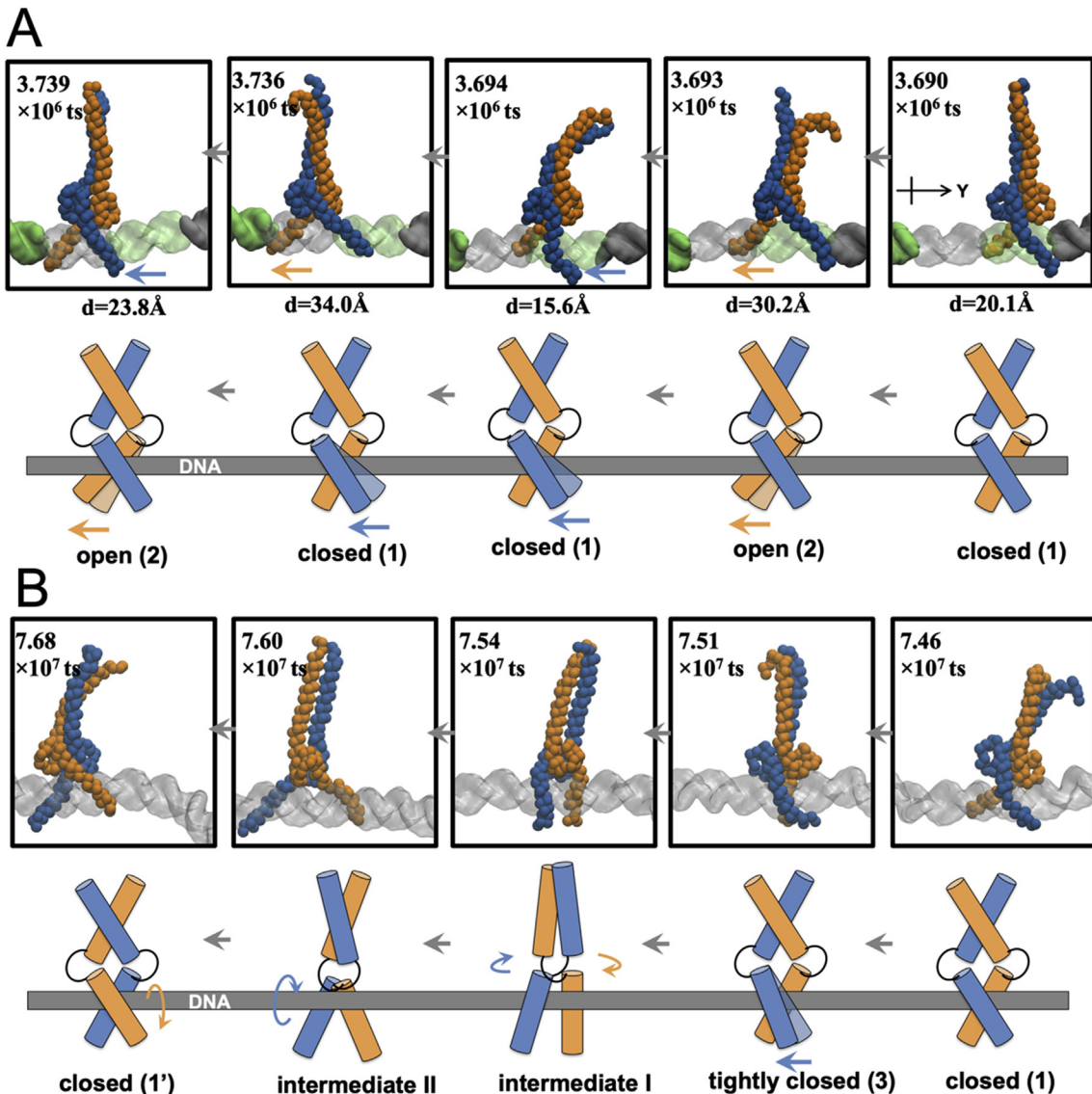


Fig. 3. An inchworm stepping model of Myc-Max diffusion on the DNA. (A) The two BRs of the Myc-Max heterodimer step along DNA. The representative snapshots are taken from the CG simulation 1 (top), with distances between the Max and Myc BRs and time steps (ts) labeled. The Myc chain is colored in blue and the Max in orange. The DNA is shown in the surface representation, colored in gray and green alternately for every 10 bp. The schematics of the Myc-Max inchworm stepping with alternating closed and open conformations are also shown (bottom). (B) The Myc-Max left-right positioning reversal or BR swapping captured in the simulation (top) and illustrated in schematics (bottom), with two closed and one tightly closed states (1, 1' and 3 in Fig. 2) and two intermediate states (I and II) presented. (For interpretation of the references to color in this figure legend, the reader is referred to the Web version of this article).

alternate stepping on the DNA, transiting between a closed and an open conformation, i.e., the leading BR steps first (from the closed to open) and the trailing BR follows (open to closed). Such inchworm stepping motions have been identified previously in nucleic acid molecular motors such as PcrA helicase [50,51] and chromatin remodeler [52].

Compared with hand-over-hand stepping motions revealed for the cytoskeleton motors myosin and kinesin, which step at about twice the inter-domain distance along the track, the step size in the inchworm protein cannot be larger than the inter-domain distance. Due to substantial electrostatic interactions at protein-DNA interface, the energy barrier for conducting the hand-over-hand protein domain motions can be significantly larger than that for the inchworm motions. Consequently, dimeric TFs and motor proteins moving along charged nucleic acid track may be more prone to the inchworm stepping than to the hand-over-hand motions.

Meanwhile, stochasticity plays a significant role in the stepping motions. Aside from random directional reversals of the protein during diffusion (i.e. forward to backward), there are occasional BR swapping that exchanges the left-right positioning of the two BRs. The swapping cannot happen, however, directly from the most stabilized closed state. Instead, a less stabilized tightly-closed state is reached first, then the BR swapping happens upon substantial rotation of the heterodimer around its own axis on the DNA, followed by conformational relaxation for the heterodimer left-right reversal.

In the inchworm stepping, Myc and Max act equally likely to be a leading chain. The left-right positioning of the heterodimer also appears equivalent. Thus, no obvious bias exists between Myc and Max as the heterodimer diffuses along the double-stranded DNA. In the atomic simulation, it has been captured that the Myc BR starts stepping on one DNA strand while dissociating from the other

strand on non-specific DNA. The HB interactions formed between Myc and the association DNA strand and that formed between Max and the complementary strand are also comparable. That is, no further bias arises between two BRs in association with DNA even when detailed protein-DNA interactions are modeled. Accordingly, the inchworm stepping revealed in the CG simulations are expected to be maintained similarly in more realistic or detailed conditions.

To maintain such inchworm motions, the 'closed-open-closed' conformational changes are essential, which highlight the closed and open conformations to be important for the Myc-Max function. The highly populated closed state presented in our CG simulations corresponds well to that being captured in the crystal structure: Two BRs bind to the two sides of a same major DNA groove, with a distance (~20 Å) in between, slightly larger than one half DNA helical pitch. The open conformation, however, has not been found yet for Myc-Max, though it shows in current CG simulations: Two BRs bind into the neighboring major and minor grooves on the DNA, respectively, with a distance (~33 Å) in between, almost a full DNA helical pitch. Opening of the Max-Max homodimer, however, have been identified recently from NMR integrated structural dynamics study [40]. In addition, a lowly populated tightly closed state of Myc-Max also appears in our simulations, which actually facilitates stochastic BR swapping for the heterodimer left-right repositioning. Accordingly, one expects that the diverse conformational states of Myc-Max can be possibly captured from high-resolution experimental detection in the future. Whether the inchworm stepping of Myc-Max along DNA impacts on its global or non-compact search dynamics in nucleus [53] can also be investigated later.

4. Methods and materials

The details of simulations settings can be found in SI.

Declaration of competing interest

The authors declare that they have no known competing financial interests or personal relationships that could have appeared to influence the work reported in this paper.

Acknowledgements

This work has been supported by NSFC Grant #11775016 and #11635002. JY has been supported by the CMCF of UCI via NSF DMS #1763272 and the Simons Foundation grant #594598 and start-up funding from UCI. We acknowledge the computational support from the Special Program for Applied Research on Super Computation of the NSFC Guangdong Joint Fund (the second phase) under Grant No. U1501501 and from the Beijing Computational Science Research Center (CSRC).

Appendix A. Supplementary data

Supplementary data to this article can be found online at <https://doi.org/10.1016/j.bbrc.2020.08.004>.

References

- [1] P.H. von Hippel, O.G. Berg, Facilitated target location in biological systems, *J. Biol. Chem.* 264 (2) (1989) 675–678.
- [2] N. Shimamoto, One-dimensional diffusion of proteins along DNA its biological and chemical significance revealed by single-molecule measurements, *J. Biol. Chem.* 274 (22) (1999) 15293–15296.
- [3] O.G. Berg, P.H. von Hippel, Selection of DNA binding sites by regulatory proteins. Statistical-mechanical theory and application to operators and promoters, *J. Mol. Biol.* 193 (1987) 723–750.
- [4] S.E. Halford, J.F. Marko, How do site-specific DNA-binding proteins find their targets? *Nucleic Acids Res.* 32 (10) (2004) 3040–3052.
- [5] M. Slusky, L.A. Mirny, Kinetics of protein-DNA interaction: facilitated target location in sequence-dependent potential, *Biophys. J.* 87 (2004) 4021–4035.
- [6] M. Bauer, R. Metzler, Generalized facilitated diffusion model for DNA-binding proteins with search and recognition states, *Biophys. J.* 102 (2012) 2321–2330.
- [7] A.A. Shvets, M.P. Kochugaeva, A.B. Kolomeisky, Mechanisms of protein search for targets on DNA: theoretical insights, *Molecules* 23 (2018) 2106.
- [8] X.S. Xie, P.J. Choi, G.-W. Li, N.K. Lee, G. Lia, Single-molecule approach to molecular biology in living bacterial cells, *Annu. Rev. Biophys.* 37 (2008) 417–444.
- [9] P.C. Blainey, G. Luo, S.C. Kou, et al., Nonspecifically bound proteins spin while diffusing along DNA, *Nat. Struct. Mol. Biol.* 16 (12) (2009) 1224.
- [10] J. Gorman, A. Plys, M.-L. Visnapuu, E. Alani, E. Greene, Visualizing the 1D diffusion of eukaryotic DNA repair factors along a chromatin lattice, *Biophys. J.* 98 (3) (2010) 591a.
- [11] A. Yildiz, J.N. Forkey, S.A. McKinney, et al., Myosin V walks hand-over-hand: single fluorophore imaging with 1.5-nm localization, *Science* 300 (5628) (2003) 2061–2065.
- [12] N. Koderer, D. Yamamoto, R. Ishikawa, T. Ando, Video imaging of walking myosin V by high-speed atomic force microscopy, *Nature* 468 (7320) (2010) 72.
- [13] C.L. Asbury, A.N. Fehr, S.M. Block, Kinesin moves by an asymmetric hand-over-hand mechanism, *Science* 302 (5653) (2003) 2130–2134.
- [14] A. Yildiz, M. Tomishige, R.D. Vale, P.R. Selvin, Kinesin walks hand-over-hand, *Science* 303 (5658) (2004) 676–678.
- [15] E.A. Abbondanzieri, W.J. Greenleaf, J.W. Shaevitz, R. Landick, S.M. Block, Direct observation of base-pair stepping by RNA polymerase, *Nature* 438 (7067) (2005) 460–465.
- [16] Y.R. Chemla, Revealing the base pair stepping dynamics of nucleic acid motor proteins with optical traps, *Phys. Chem. Chem. Phys.* 12 (13) (2010) 3080–3095.
- [17] M. Schlierf, G. Wang, X.S. Chen, T. Ha, Hexameric helicase G40P unwinds DNA in single base pair steps, *Elife* 8 (2019), e42001.
- [18] Q. Liao, M. Lüking, D.M. Krüger, et al., Long time-scale Atomistic simulations of the structure and dynamics of transcription factor-DNA recognition, *J. Phys. Chem. B* 123 (17) (2019) 3576–3590.
- [19] J.L. Klepeis, K. Lindorff-Larsen, R.O. Dror, D.E. Shaw, Long-timescale molecular dynamics simulations of protein structure and function, *Curr. Opin. Struct. Biol.* 19 (2) (2009) 120–127.
- [20] J.R. Perilla, B.C. Goh, C.K. Cassidy, et al., Molecular dynamics simulations of large macromolecular complexes, *Curr. Opin. Struct. Biol.* 31 (2015) 64–74.
- [21] O. Givaty, Y. Levy, Protein sliding along DNA: dynamics and structural characterization, *J. Mol. Biol.* 385 (4) (2009) 1087–1097.
- [22] T. Terakawa, H. Kenzaki, S. Takada, p53 searches on DNA by rotation-uncoupled sliding at C-terminal tails and restricted hopping of core domains, *J. Am. Chem. Soc.* 134 (35) (2012) 14555–14562.
- [23] A. Marcovitz, Y. Levy, Frustration in protein–DNA binding influences conformational switching and target search kinetics, *Proc. Natl. Acad. Sci. Unit. States Am.* 108 (44) (2011) 17957–17962.
- [24] S. Takada, R. Kanada, C. Tan, T. Terakawa, W. Li, H. Kenzaki, Modeling structural dynamics of biomolecular complexes by coarse-grained molecular simulations, *Acc. Chem. Res.* 48 (12) (2015) 3026–3035.
- [25] H. Kenzaki, N. Koga, N. Hori, et al., CafeMol: a coarse-grained biomolecular simulator for simulating proteins at work, *J. Chem. Theor. Comput.* 7 (6) (2011) 1979–1989.
- [26] G.S. Freeman, D.M. Hinckley, J.J. de Pablo, A coarse-grain three-site-per-nucleotide model for DNA with explicit ions, *J. Chem. Phys.* 135 (16) (2011) 10B625.
- [27] T. Ando, J. Skolnick, Sliding of proteins non-specifically bound to DNA: brownian dynamics studies with coarse-grained protein and DNA models, *PLoS Comput. Biol.* 10 (12) (2014).
- [28] T. Niina, G.B. Brandani, C. Tan, S. Takada, Sequence-dependent nucleosome sliding in rotation-coupled and uncoupled modes revealed by molecular simulations, *PLoS Comput. Biol.* 13 (12) (2017), e1005880.
- [29] K.B. Marcu, S.A. Bosone, A.J. Patel, Myc function and regulation, *Annu. Rev. Biochem.* 61 (1) (1992) 809–858.
- [30] M.D. Cole, S.B. McMahon, The Myc oncoprotein: a critical evaluation of transactivation and target gene regulation, *Oncogene* 18 (19) (1999) 2916–2924.
- [31] C.V. Dang, MYC on the path to cancer, *Cell* 149 (1) (2012) 22–35.
- [32] E.M. Blackwood, R.N. Eisenman, Max: a helix-loop-helix zipper protein that forms a sequence-specific DNA-binding complex with Myc, *Science* 251 (4998) (1991) 1211–1217.
- [33] B. Amati, S. Dalton, M.W. Brooks, T.D. Littlewood, G.I. Evan, H. Land, Transcriptional activation by the human c-Myc oncoprotein in yeast requires interaction with Max, *Nature* 359 (6394) (1992) 423–426.
- [34] L. Kretzner, E.M. Blackwood, R.N. Eisenman, Myc and Max proteins possess distinct transcriptional activities, *Nature* 359 (6394) (1992) 426–429.
- [35] A. Sabò, B. Amati, Genome recognition by MYC, *Cold Spring Harbor perspectives in medicine* 4 (2) (2014) a014191.
- [36] M. Conacci-Sorrell, L. McMerrin, R.N. Eisenman, An overview of MYC and its interactome, *Cold Spring Harbor perspectives in medicine* 4 (1) (2014), a014357.
- [37] M.-E. Beaulieu, F. Castillo, L. Soucek, Structural and biophysical insights into

the function of the intrinsically disordered Myc oncoprotein, *Cells* 9 (4) (2020) 1038.

[38] S.K. Nair, S.K. Burley, X-ray structures of Myc-Max and Mad-Max recognizing DNA: molecular bases of regulation by proto-oncogenic transcription factors, *Cell* 112 (2) (2003) 193–205.

[39] A.R. Ferré-D'Amré, G.C. Prendergast, E.B. Ziff, S.K. Burley, Recognition by Max of its cognate DNA through a dimeric b/HLH/Z domain, *Nature* 363 (6424) (1993) 38–45.

[40] G. Sicoli, H. Vezin, K. Ledolter, T. Kress, Kurzbach DJNar, Conformational tuning of a DNA-bound transcription factor 47 (10) (2019) 5429–5435.

[41] L.A. Carabet, P.S. Rennie, A. Cherkasov, Therapeutic inhibition of Myc in cancer. Structural bases and computer-aided drug discovery approaches, *Int. J. Mol. Sci.* 20 (1) (2019) 120.

[42] C. Yu, X. Niu, F. Jin, Z. Liu, C. Jin, L. Lai, Structure-based inhibitor design for the intrinsically disordered protein c-Myc, *Sci. Rep.* 6 (1) (2016) 1–11.

[43] G. Mustata, A.V. Follis, D.I. Hammoudeh, et al., Discovery of novel Myc–Max heterodimer disruptors with a three-dimensional pharmacophore model, *J. Med. Chem.* 52 (5) (2009) 1247–1250.

[44] P. Lavigne, L.H. Kondejewski, M.E. Houston Jr, et al., Preferential heterodimeric parallel coiled-coil formation by synthetic Max and c-Myc leucine zippers: a description of putative electrostatic interactions responsible for the specificity of heterodimerization, *J. Mol. Biol.* 254 (3) (1995) 505–520.

[45] F. Lorenzin, U. Benay, A. Baluapuri, et al., Different promoter affinities account for specificity in MYC-dependent gene regulation, *Elife* 5 (2016), e15161.

[46] W. Hua, J. Chung, J. Gelles, Distinguishing inchworm and hand-over-hand processive kinesin movement by neck rotation measurements, *Science* 295 (5556) (2002) 844–848.

[47] H. Flechsig, A.S. Mikhailov, Simple mechanics of protein machines, *J. R. Soc. Interface* 16 (155) (2019) 20190244.

[48] C. Clementi, H. Nymeyer, J.N. Onuchic, Topological and energetic factors: what determines the structural details of the transition state ensemble and “en-route” intermediates for protein folding? An investigation for small globular proteins, *J. Mol. Biol.* 298 (5) (2000) 937–953.

[49] O. Ecevit, M.A. Khan, D.J. Goss, Kinetic analysis of the interaction of b/HLH/Z transcription factors Myc, Max, and Mad with cognate DNA, *Biochemistry* 49 (12) (2010) 2627–2635.

[50] J. Yu, T. Ha, K. Schulten, Structure-based model of the stepping motor of PcrA helicase, *Biophys. J.* 91 (6) (2006) 2097–2114.

[51] J. Yu, T. Ha, K. Schulten, How directional translocation is regulated in a DNA helicase motor, *Biophys. J.* 93 (11) (2007) 3783–3797.

[52] G.B. Brandani, S. Takada, Chromatin remodelers couple inchworm motion with twist-defect formation to slide nucleosomal DNA, *PLoS Comput. Biol.* 14 (11) (2018), e1006512.

[53] I. Izeddin, V. Récamier, L. Bosanac, et al., Single-molecule tracking in live cells reveals distinct target-search strategies of transcription factors in the nucleus, *Elife* 3 (2014), e02230.